



Marchena-Menéndez, J., Ramírez-Torres, A., Penta, R., Rodríguez-Ramos, R. and Merodio, J. (2019) Macroscopic thermal profile of heterogeneous cancerous breasts. A three-dimensional multiscale analysis. *International Journal of Engineering Science*, 144, 103135. (doi: [10.1016/j.ijengsci.2019.103135](https://doi.org/10.1016/j.ijengsci.2019.103135))

There may be differences between this version and the published version. You are advised to consult the publisher's version if you wish to cite from it.

<http://eprints.gla.ac.uk/213045/>

Deposited on 31 March 2020

Enlighten – Research publications by members of the University of Glasgow
<http://eprints.gla.ac.uk>

Manuscript Details

Manuscript number	IJES_2019_496
Title	Macroscopic thermal profile of heterogeneous cancerous breasts. A three-dimensional multiscale analysis
Article type	Full Length Article

Abstract

The present work focuses on the multiscale analysis of temperature maps for cancerous breasts. A three-dimensional model is proposed based on a system of bioheat transfer equations for the healthy and cancerous breast regions, which are characterized by different microstructure and thermophysical properties. The geometrical model of the cancerous breast is identified by the presence of muscle, glandular and fat tissues, as well as the heterogeneous tumor tissue. The latter is assumed to be a two-phase periodic composite with a spherical inclusion. A cubic lattice distribution is chosen, wherein the constituents exhibit isotropic thermal conductivity behavior. The tissue effective thermal conductivities are computed by means of the asymptotic homogenization approach, i.e. by solving relevant periodic problems on the cell which is representative of the malignant tissue microstructure. These are then exploited to solve the macroscale homogenized model by finite elements. The obtained results in terms of temperature maps are successfully compared with relevant experiments and could pave the way towards the development of a robust multiscale mathematical framework featuring microstructural information which can be useful in cancer diagnosis. This approach could provide qualitative and quantitative hints that can be used to improve tumor detection based on temperature maps of the breast tissue.

Keywords	Asymptotic homogenization; Cancerous breast; Bioheat equation.
Manuscript category	Solids and Materials
Corresponding Author	Reinaldo Rodriguez-Ramos
Corresponding Author's Institution	Universidad de La Habana
Order of Authors	Jorge Marchena-Menéndez, Ariel Ramírez Torres, Raimondo Penta, Reinaldo Rodriguez-Ramos, Jose Merodio

Submission Files Included in this PDF

File Name [File Type]

cover_letter.pdf [Cover Letter]

Title_without_authors.pdf [Title Page (with Author Details)]

IJES_07_03_2019_without_authors.pdf [Manuscript (without Author Details)]

To view all the submission files, including those not included in the PDF, click on the manuscript title on your EVISE Homepage, then click 'Download zip file'.

Dr. Igor Sevostianov

Editor Special Issue

International Journal of Engineering Science

Dear Prof. Sevostianov,

I would like to submit to your journal the contribution entitled "Macroscopic thermal profile of heterogeneous cancerous breasts. A three-dimensional multiscale analysis" by J. Marchena-Menéndez, A. Ramírez-Torres, R. Penta, R. Rodríguez-Ramos, J. Merodio.

The present work focuses on the multiscale analysis of temperature maps for cancerous breasts. A three-dimensional model is proposed based on a system of bioheat transfer equations for the healthy and cancerous breast regions, which are characterized by different microstructure and thermophysical properties. The geometrical model of the cancerous breast is identified by the presence of muscle, glandular and fat tissues, as well as the heterogeneous tumor tissue. The latter is assumed to be a two-phase periodic composite with a spherical inclusion. A cubic lattice distribution is chosen, wherein the constituents exhibit isotropic thermal conductivity behavior. The tissue effective thermal conductivities are computed by means of the asymptotic homogenization approach, i.e. by solving relevant periodic problems on the cell which is representative of the malignant tissue microstructure. These are then exploited to solve the macroscale homogenized model by finite elements. The obtained results in terms of temperature maps are successfully compared with relevant experiments and could pave the way towards the development of a robust multiscale mathematical framework featuring microstructural information which can be useful in cancer diagnosis. This approach could provide qualitative and quantitative hints that can be used to improve tumor detection based on temperature maps of the breast tissue.

Sincerely yours,

Reinaldo Rodriguez-Ramos (Corresponding author)

reinaldo@matcom.uh.cu

"Macroscopic thermal profile of heterogeneous cancerous breasts. A three-dimensional multiscale analysis".

The present work focuses on the multiscale analysis of temperature maps for cancerous breasts. A three-dimensional model is proposed based on a system of bioheat transfer equations for the healthy and cancerous breast regions, which are characterized by different microstructure and thermophysical properties. The geometrical model of the cancerous breast is identified by the presence of muscle, glandular and fat tissues, as well as the heterogeneous tumor tissue. The latter is assumed to be a two-phase periodic composite with a spherical inclusion. A cubic lattice distribution is chosen, wherein the constituents exhibit isotropic thermal conductivity behavior. The tissue effective thermal conductivities are computed by means of the asymptotic homogenization approach, i.e. by solving relevant periodic problems on the cell which is representative of the malignant tissue microstructure. These are then exploited to solve the macroscale homogenized model by finite elements. The obtained results in terms of temperature maps are successfully compared with relevant experiments and could pave the way towards the development of a robust multiscale mathematical framework featuring microstructural information which can be useful in cancer diagnosis. This approach could provide qualitative and quantitative hints that can be used to improve tumor detection based on temperature maps of the breast tissue.

Macroscopic thermal profile of heterogeneous cancerous breasts. A three-dimensional multiscale analysis

Abstract

The present work focuses on the multiscale analysis of temperature maps for cancerous breasts. A three-dimensional model is proposed based on a system of bioheat transfer equations for the healthy and cancerous breast regions, which are characterized by different microstructure and thermophysical properties. The geometrical model of the cancerous breast is identified by the presence of muscle, glandular and fat tissues, as well as the heterogeneous tumor tissue. The latter is assumed to be a two-phase periodic composite with a spherical inclusion. A cubic lattice distribution is chosen, wherein the constituents exhibit isotropic thermal conductivity behavior. The tissue effective thermal conductivities are computed by means of the asymptotic homogenization approach, i.e. by solving relevant periodic problems on the cell which is representative of the malignant tissue microstructure. These are then exploited to solve the macroscale homogenized model by finite elements. The obtained results in terms of temperature maps are successfully compared with relevant experiments and could pave the way towards the development of a robust multiscale mathematical framework featuring microstructural information which can be useful in cancer diagnosis. This approach could provide qualitative and quantitative hints that can be used to improve tumor detection based on temperature maps of the breast tissue.

Keywords: Asymptotic homogenization, Cancerous breast, Bioheat equation

1. Introduction

Cancer is the second leading cause of death worldwide and breast cancer is one of the most frequently diagnosed. Fibroadenoma is one of the most common types of breast cancer found in adolescents and it has been found that its presence tends to raise the breast surface temperature in an abnormal way, so it could be detected using thermal imaging [1]. Even though mammography and ultrasound are frequently used clinical protocols to detect and provide a diagnosis of breast cancer, other techniques, such as clinical examination and thermography, are also employed to identify breast cancer. Mammography is considered the standard procedure for detecting breast cancer, yet it is less effective for recognizing tumors in dense breasts. For instance, it is less sensitive in detecting tumors in woman with dense breast tissue and implants, there is a risk of rupture of tumors encapsulation (as the process of taking a mammogram involves the compression of the breast tissue) and also, confers a slightly increased risk of causing radiation induced breast cancer. Thermal imaging has the potential to be a noninvasive and effective technique for early breast cancer screening (see e.g. [2, 3, 4]).

A combination of therapies that incorporates thermography may boost both sensitivity and specificity. In several works, the temperature distributions over breasts with and without tumors have been

studied, wherein heat transfer in the biological tissue is modeled using Pennes bioheat equation [?]. For instance, There exist recent works dealing with heat transfer in complex multiscale tumors, such as [5], [6] and [7]. In [7] the authors take into account the heterogeneity of the tumor and studied its influence on the breast surface temperature for a particular two-dimensional cross-section geometry. In the present work, we generalize the results given in [7] by introducing a three-dimensional model for the cancerous tissue.

2. Statement of the problem

We will work with a three-dimensional breast geometry. The healthy breast will be represented by three homogeneous tissues: glandular, muscle and fat tissues represented by Ω_g , Ω_m and Ω_f , respectively with Lipschitz boundary $\partial\Omega = \partial\Omega^n \cup \partial\Omega^d$, being $\partial\Omega^n$ and $\partial\Omega^d$ the muscle and fat external boundaries, where $\partial\Omega^n \cap \partial\Omega^d = \emptyset$ (see Fig. 1). On the other hand, the cancerous tissue will be characterized by two regions of dissimilar thermal properties: the tumoral area (Ω_t^ε) and the glandular area (Ω_g^ε). In this sense, the cancerous region will consist of a periodic microstructure associated with the open, bounded, and connected domain $\Omega_\varepsilon = \Omega_g^\varepsilon \cup \Omega_t^\varepsilon \cup \partial\Omega_g^\varepsilon$ with Lipschitz boundary $\partial\Omega_\varepsilon = \partial\Omega_g^\varepsilon$ and with $\Omega_g^\varepsilon \cap \Omega_t^\varepsilon = \emptyset$. Hence, the cancerous breast is represented by $\Omega = \Omega_f \cup \Omega_m \cup \Omega_g \cup \Omega_\varepsilon$ (Fig. 1). Moreover, let $\varepsilon > 0$ be the size of the microstructure and $\mathbf{y} = \mathbf{x}/\varepsilon$ the fast scale coordinate. The microscopic periodic cell is denoted with \mathbf{Y} . The portion of the glandular tissue contained in \mathbf{Y} is indicated by \mathbf{Y}_g , while \mathbf{Y}_t represents the inclusions (conformed by a cylinder, a disc, a sphere, an ellipsoid, and three orthogonal fibers) in \mathbf{Y} , with Lipschitz boundary $\partial\mathbf{Y}_t$ such that $\mathbf{Y} = \mathbf{Y}_g \cup \mathbf{Y}_t \cup \partial\mathbf{Y}_t$, with $\bar{\mathbf{Y}}_t \subset \mathbf{Y}$ and $\mathbf{Y}_g \cap \mathbf{Y}_t = \emptyset$. It is also assumed that Ω_g^ε is connected and that the inclusions do not intersect the boundary $\partial\Omega_g^\varepsilon$. In previous works, soft tissues assume to present this type of arrangement.

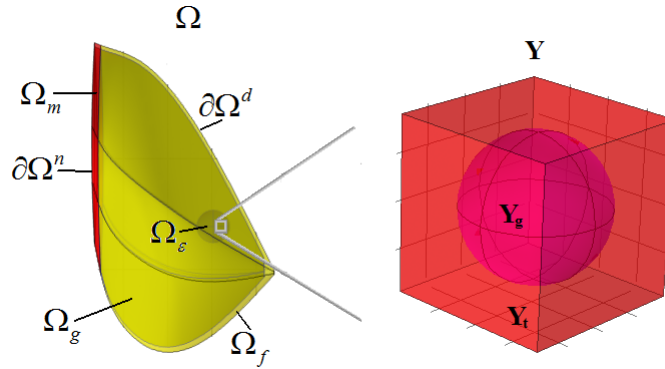


Figure 1: Decomposition of the macroscopic three-dimensional domain (left) and the corresponding unit periodic cell (right).

The following bioheat transfer equations (Pennes, 1948) provides a way to model the stationary temperature fields u and u_ε

$$(P^p) \quad - \frac{\partial}{\partial x_i} \left(K_{ij}^p \frac{\partial u}{\partial x_j} \right) + \rho_b c_b \omega_b^p u = q_m^p + \rho_b c_b \omega_b^p u_a \quad \text{in } \Omega_p \quad (1)$$

where the sub-index $p = f, g, m, \varepsilon$ indicates the region over which every variable is defined. Moreover u_a is the arterial blood temperature, $K_{ij}^p = \kappa_p \delta_{ij}$ denotes the tissues thermal conductivity, ρ_b is the blood mass density, c_b the blood specific heat capacity, ω_b^p the blood perfusion and q_m^p the metabolic heat generation for each region Ω_p .

Boundary conditions for equation (1) for $p = f, m$ are heat transfer by convection between the surface of the tissue and the external environment on $\partial\Omega^n$ and a prescribed temperature value on $\partial\Omega^d$.

$$-K_{ij}^p \frac{\partial u}{\partial x_j} n_i = h(u - u_e) \quad \text{in } \partial\Omega^n \quad (2)$$

$$u = u_c \quad \text{in } \partial\Omega^d \quad (3)$$

In (2), u_c is the temperature at the boundary between breast and chest, u_e is the surrounding temperature and h represents the combined effective heat transfer coefficient due to convection, radiation and evaporation of $13,5W/m^2C$ [8]. Also, we consider an ideal contact between the glandular and tumorous tissue, so that we prescribe heat and temperature continuity on $\partial\Omega_\varepsilon$ and $\partial\Omega_g$. Moreover, for the case of $p = \varepsilon$ continuity conditions for temperature and heat flow are imposed on Γ^ε (boundary between the glandular tissue Ω_g^ε and the tumor inclusions Ω_t^ε), i.e.,

$$[[u^\varepsilon]] = 0 \quad \text{on } \Gamma^\varepsilon, \quad (4)$$

$$[[K_{ij}^\varepsilon \frac{\partial u^\varepsilon}{\partial x_j} n_i]] = 0 \quad \text{on } \Gamma^\varepsilon, \quad (5)$$

where the operator $[[\cdot]]$ indicates denotes the jump across the interface between the constituents in the heterogeneous region.

Besides, the rapidly oscillating coefficients $K_{ij}^\varepsilon, \rho_b^\varepsilon, c_b^\varepsilon, \omega_b^\varepsilon$ and q_m^ε are defined as follows

$$K_{ij}^\varepsilon(x) = \begin{cases} \kappa_g \delta_{ij}, & x \in \Omega_g^\varepsilon, \\ \kappa_t \delta_{ij}, & x \in \Omega_t^\varepsilon, \end{cases} \quad \omega_b^\varepsilon(x) = \begin{cases} \omega_b^g, & x \in \Omega_g^\varepsilon, \\ \omega_b^t, & x \in \Omega_t^\varepsilon, \end{cases} \quad q_m^\varepsilon(x) = \begin{cases} q_m^g, & x \in \Omega_g^\varepsilon, \\ q_m^t, & x \in \Omega_t^\varepsilon. \end{cases} \quad (6)$$

3. Two-Scale Asymptotic Homogenization

Here, the two-scale asymptotic homogenization technique ([9, 10]) is applied to find the homogenized solution of Eq. (1) for $p = \varepsilon$. Specifically, an asymptotic expansion of u^ε is sought as a function of ε for $\varepsilon \rightarrow 0$, namely

$$u^\varepsilon(x) = u^{(0)}(x, y) + \varepsilon u^{(1)}(x, y) + \varepsilon^2 u^{(2)}(x, y) + \dots \quad (7)$$

It can be verified that $u^{(0)}$ does not depend on the fast variable, i.e. $u^{(0)} = u^{(0)}(x)$. Furthermore, $u^{(1)}(x, y)$ can be written as $u^{(1)}(x, y) = \chi_l(y) \frac{\partial u^{(0)}(x)}{\partial x_l}$, where $\chi_l(y)$ is periodic in y . In particular, the

vector function $\chi(y)$ satisfies the following unit cell problem

$$-\frac{\partial}{\partial y_i} \left(K_{ij}(y) \frac{\partial \chi_l(y)}{\partial y_j} + K_{il}(y) \right) = 0 \quad \text{in } \mathbf{Y} \setminus \Gamma, \quad (8)$$

$$[[\chi_l]] = 0 \quad \text{on } \Gamma, \quad (9)$$

$$\left[\left(K_{ij}(y) \frac{\partial \chi_l(y)}{\partial y_j} + K_{il}(y) \right) n_i \right] = 0 \quad \text{on } \Gamma \quad (10)$$

and $u^{(0)}(x)$ the solution of the homogenized problem (see for more details Ramirez-Torres et al. (2017b))

$$-\frac{\partial}{\partial x_i} \left(\hat{K}_{ij} \frac{\partial u^{(0)}(x)}{\partial x_j} \right) + \hat{g} u^{(0)}(x) = \hat{f} \quad \text{in } \Omega_\varepsilon, \quad (11)$$

$$u^{(0)}(x) = u_g \quad \text{on } \partial\Omega_\varepsilon, \quad (12)$$

where

$$\hat{g} = \rho_b c_b \omega_b^g \frac{|\mathbf{Y}_g|}{|\mathbf{Y}|} + \rho_b c_b \omega_b^t \frac{|\mathbf{Y}_t|}{|\mathbf{Y}|}, \quad (13)$$

$$\hat{f} = (q_m^g + \rho_b c_b \omega_b^g u_a) \frac{|\mathbf{Y}_g|}{|\mathbf{Y}|} + (q_m^t + \rho_b c_b \omega_b^t u_a) \frac{|\mathbf{Y}_t|}{|\mathbf{Y}|}, \quad (14)$$

and $|\mathbf{Y}_\alpha|$ with $\alpha = g, t$ represents the volume fraction of the glandular or tumor cell portion, respectively.

The effective constant coefficients \hat{K}_{il} are given by

$$\hat{K}_{il} = \left\langle K_{ij} \frac{\partial \chi_l}{\partial y_j} + K_{il} \right\rangle, \quad (15)$$

where $\langle \cdot \rangle = \frac{1}{|\Omega|} \int_\Omega (\cdot)$ denotes the volume average operator.

3.1. Weak formulations of the homogenized and homogeneous problems

We notice that the numerical solution of the cell problem is found by using COMSOL packages. However, the solutions homogenized and homogeneous problems are computed via the finite element method (FEM) by using their weak formulation. In this sense, we follow the approach depicted in [7, 11] and introduce the weak formulation for each P^p ($p = f, g, m$) as

$$\begin{cases} \text{Find } \tilde{u} \in H_d^1(\Omega_p) \text{ such that} \\ a(\tilde{u}, v) = L(v), \quad \forall v \in H_d^1(\Omega_p), \end{cases} \quad (16)$$

where $H_d^1(\Omega_p) = \{u \in H^1(\Omega_p) \text{ s.t. } \gamma(u) = 0 \text{ on } \partial\Omega_p^d\}$ and γ denotes the trace operator. Moreover,

$$a(\tilde{u}, v) = \int_{\Omega_p} \mathbf{K}^p \nabla_x \tilde{u} \cdot \nabla_x v dx + \int_{\Omega_p} g^p \tilde{u} v dx + \int_{\partial\Omega_p^n} h \tilde{u} v dS, \quad (17)$$

$$L(v) = \int_{\Omega_p} f^p v dx - \int_{\Omega_p} g^p (R_0 u_c) v dx - \int_{\Omega_p} \mathbf{K}^p \nabla (R_0 u_c) \cdot \nabla_x v dx + \int_{\partial\Omega_p^n} h (u_e - R_0 u_c) v dS. \quad (18)$$

	Muscle	Gland	Fat	Tumor
$\kappa(W/m^{\circ}C)$	0.48	0.48	0.21	0.511
$\omega(1/s)$	0.0009	0.000539	0.0002	0.0108
$c_b(J/kg^{\circ}C)$	4200			
$\rho_b(kg/m^3)$	1060			
$q_m(Wm^{-3})$	700	700	400	

Table 1: Thermophysical Parameters. The blood density ρ_b and specific heat capacity c_b do not depend on the actual domain of investigation as they refer to the blood and they are considered constants here.

Furthermore, following a similar analysis the weak formulation of the homogenized problem given by equations (11) and (12) is

$$\begin{cases} \text{Find } \tilde{u}^{(0)} \in H_d^1(\Omega_\varepsilon) \text{ such that} \\ a(\tilde{u}^{(0)}, v) = L(v), \quad \forall v \in H_d^1(\Omega_\varepsilon), \end{cases} \quad (19)$$

where,

$$a(\tilde{u}^{(0)}, v) = \int_{\Omega_\varepsilon} \hat{\mathbf{K}} \nabla_x \tilde{u}^{(0)} \cdot \nabla_x v dx + \int_{\Omega_\varepsilon} \hat{g} \tilde{u}^{(0)} v dx, \quad (20)$$

$$L(v) = \int_{\Omega_\varepsilon} \hat{f} v dx - \int_{\Omega_\varepsilon} \hat{\mathbf{K}} \nabla_x (R_0 u_g) \cdot \nabla_x v dx - \int_{\Omega_\varepsilon} \hat{g} (R_0 u_g) v dx. \quad (21)$$

Proof of existence and uniqueness of solutions to previous problem formulations can be found in [12].

4. Results and discussions

In the present section, we compare the resulting thermal distribution of a cancerous breast with respect to a healthy one. Furthermore, we show how the position and size of the tumorous region changes the breast thermal profile. The thermophysical parameters used in this work were taken from [13, 14, 15, 16] and are reported in Table 1.

In particular, the data presented in Table 1 for the tumor and the glandular tissues refer to the specific portion that they occupy in the heterogeneous domain Ω_ε and not to the entire tumor region. Moreover, temperatures are fixed as $u_e = u_a = 36^{\circ}C$ [14]. The surrounding temperature is fixed to $u_c = 26^{\circ}C$. The metabolic heat value for different tumor sizes follows the law given in [5] as $q_m^t = C/(468.6 \ln(100D) + 50)$, where $C = 3.27 \times 10^6 Wday/m^3$ and D refers to the tumor diameter. For a 45% of volume fraction the effective thermal conductivity of the heterogeneous tumor inclusion obtained is $\hat{\kappa} = 0.497 W/m^{\circ}C$. Moreover, $\hat{g} = 27698 W/m^3K$ and $\hat{f} = 8599200 W/m^3K$.

In Figure 2, we present the temperature distribution of a cancerous breast (panel on the left) and a healthy one (panel on the right). We note that, an anomaly on the thermal profile arises with the presence of a tumor. This phenomenon has been reported by experimental studies. As reported in

several works (see e.g. [14, 5, 7]) the breast surface temperature increases when the tumor is closer to its boundary.

Figure 3 do actually shows how the present model is able to infer this phenomenon on the idealized breast surface. Now, we analyze the temperature difference between normal and cancerous breasts over the upper surface of the breast.

Figures 4 and 5 show how the tumor depth has a greater influence on the breast thermal profile than tumor size. These phenomena has also been observed in other studies ([5, 7]).

In addition, in Figure 6 it can be noted that the cancer volume fraction in the malignant region affects the breast surface temperature. Even though the local problem geometry does not allow to do an analysis for high volume fractions, it can be seen how, the breast surface temperature increases at the same time that the glandular portion occupies a smaller domain in the malignant region.

Finally, Figure 7 shows the comparison of the presented model versus the experimental data reported in [17] where h , d , u_a , and u_c were fixed to $10 \text{ W/m}^\circ\text{C}$, 20 mm , 36°C , 26°C , respectively. We note that d refers to the tumorous region’s diameter. For such a comparison, a cross-section of the breast was taken into account. It can be observed a small quantitatively difference and a very good qualitative match in the whole interval. Changes in the subcutaneous fat layer and muscle layer, as a bigger volume fraction in the local problem for the tumorous region homogenization must improve the result matching.

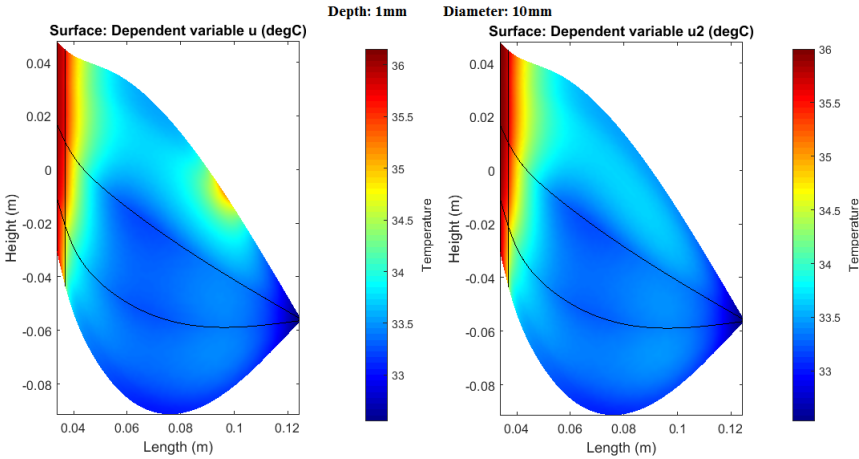


Figure 2: Breast surface temperature comparison. Breast with tumor (left) and healthy breast (right).

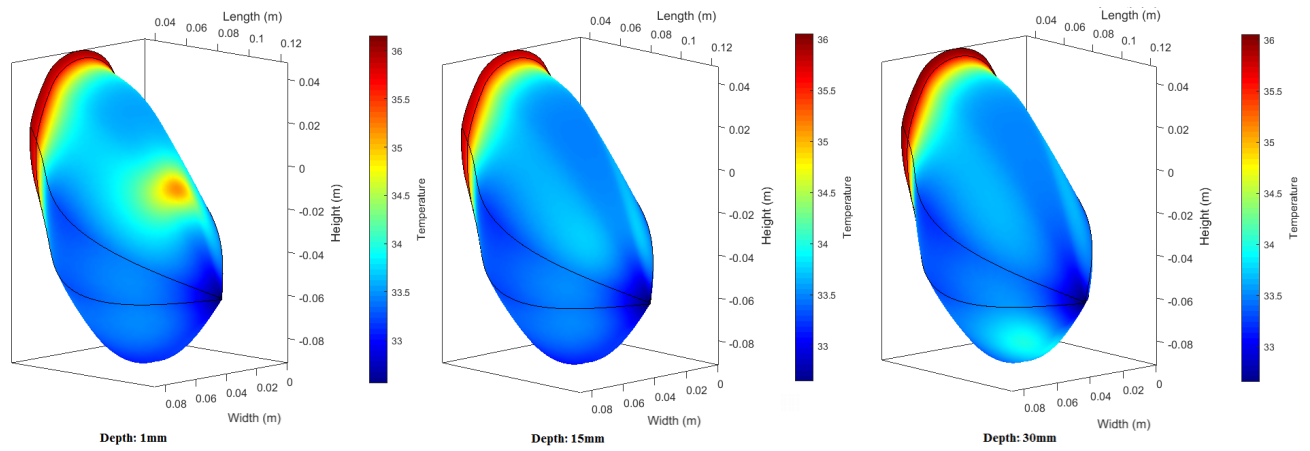


Figure 3: Thermal field for a breast with a tumor of 10 mm in its diameter at different depths.

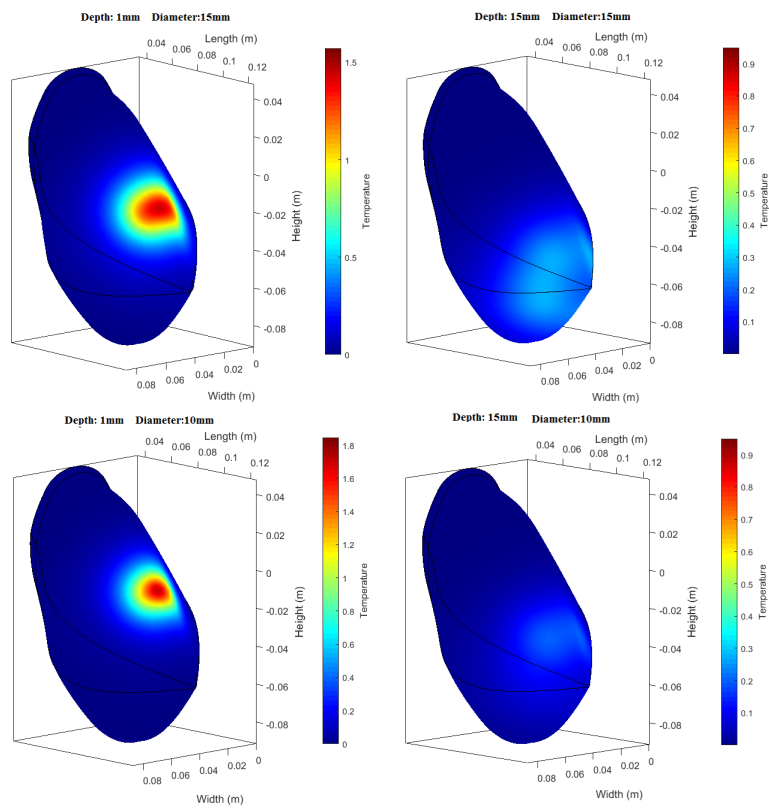


Figure 4: Temperature difference between normal and cancerous breasts for different tumor radiuses and depths.

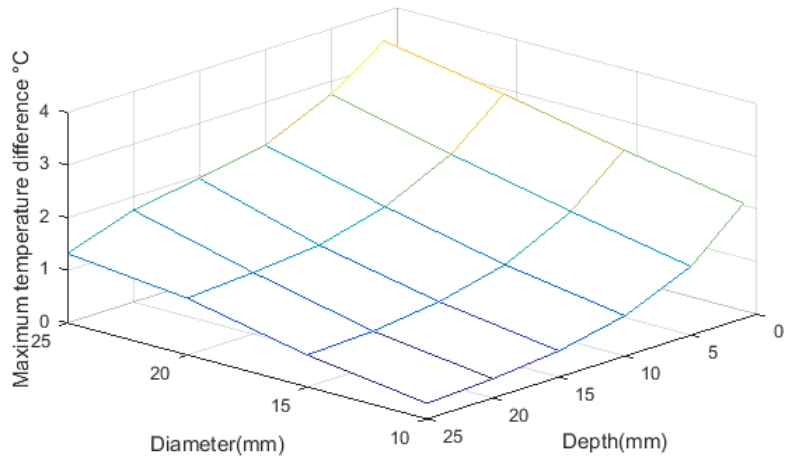


Figure 5: Maximum temperature difference between normal and cancerous breasts for different tumor radiuses and depths.

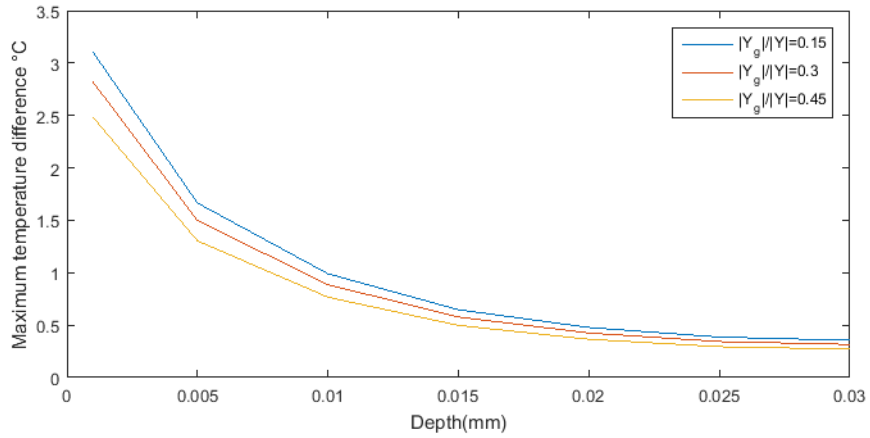


Figure 6: Maximum temperature difference between normal and cancerous breasts. The figure shows how the maximum temperature difference increases for smaller volume fractions of the glandular with respect to the tumor location from the breast surface.

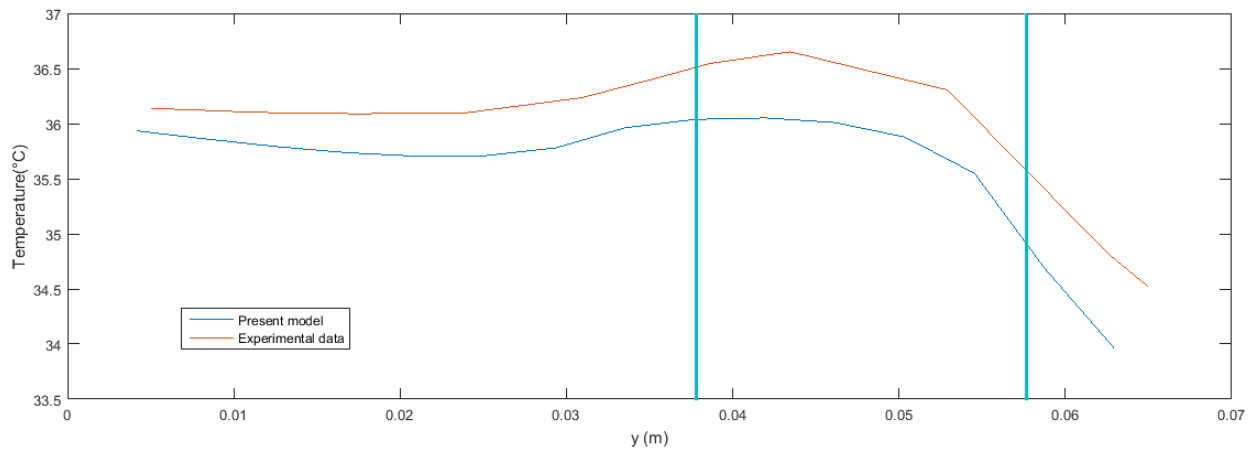


Figure 7: Comparison of numerical results from the present model with the experimental data taken from [17].

5. Conclusions

The present work concerns the analysis of the temperature distribution for cancerous breasts. The results are obtained via three-dimensional numerical simulations of macroscopic bioheat-type equations, where the thermal conductivities are computed via solving three-dimensional periodic cell problems on the tumor microstructure, as prescribed by the asymptotic homogenization approach. Our results are in substantial agreement with past works where the analysis was conducted in two dimensions. However, an important advantage when performing a fully three-dimensional analysis is the fact that temperature changes can be studied on the whole breast surface, so that the results are more likely to be significant and relevant in terms of tumor detection. Our analysis is in good qualitative agreement with the experimental results and focuses on the influence of the position and size of the cancerous region, as well as the volume fraction of the tumor, on the breast surface thermal field. Our results suggest that the tumor position affects the temperature maps more than its volume fraction, and provide a preliminary basis for future three-dimensional studies aimed at providing hints towards cancer detection. The next natural step is the extension of the present model to more realistic geometries and physical features, such as the tumor vascularization. Numerical simulations of the present model extended to vascularized tumors (see also the theoretical works and their numerical results reported in [21, 18, 19, 20], respectively, for cancer blood and drug flow maps) will provide more realistic results in elucidating the role of the microvascular geometry and functionalities on cancer temperature maps.

Acknowledgments

ART acknowledges the Dipartimento di Scienze Matematiche (DISMA) “G.L. Lagrange” of the Politecnico di Torino, “Dipartimento di Eccellenza 2018–2022” (‘Department of Excellence 2018–2022’). RR thanks to Departamento de Matemática y Mecánica- IIMAS and PREI-DGAPA, UNAM Mexico for the support and also to Ana Arteaga, Ramiro Chávez for the computational assistance.

References

- [1] Salhab, M., Keith, L. G., Laguens, M., Reeves, W. and Mokbel, K., 2006, *The potential role of dynamic thermal analysis in breast cancer detection. International Seminars in Surgical Oncology*, 5, pp.1-5.
- [2] Ng, E.Y.K., 2008, *A Review of Thermography as Promising Noninvasive Detection Modality for Breast Tumor*, International Journal of Thermal Sciences, vol. 48, pp. 849-859.
- [3] J.-L. Gonzalez-Hernandez, A. N. Recinella, S. G. Kandlikar, D. Dabydeen, L. Medeiros, P. Phatak, 2019. *Technology, application and potential of dynamic breast thermography for the detection of breast cancer*. International Journal of Heat and Mass Transfer 131:558-573.
- [4] PR Pavithra, KS Ravichandran, KR Sekar, R Manikandan, 2018, *The Effect of Thermography on Breast Cancer Detection*. Sys Rev Pharm. 9:10-16.
- [5] Jiang, L., Zhan, W. and Loew, M.H., 2011. *Modeling static and dynamic thermography of the human breast under elastic deformation*, Phys. Med. Biol. 56 (1), pp. 187-202.

- [6] Nabil, M., P. Decuzzi, and Paolo Zunino. *Modelling mass and heat transfer in nano-based cancer hyperthermia*. Royal Society open science 2.10 (2015): 150447.
- [7] Ramírez-Torres, A., Rodríguez-Ramos, R., Sabina, F. J., García-Reimbert, C., Penta, R., Merodio, J., Guinovart-Díaz, R., Bravo-Castillero, J., Conci, A. and Preziosi, L., 2017, *The role of malignant tissue on the thermal distribution of cancerous breast*, Journal of Theoretical Biology, 426, pp. 152-161.
- [8] Wahab, A.A., Salim, M.I.M., Ahamat, M.A., Manaf, N.A., Yunus, J. and Lai, K.W., 2015, *Thermal distribution analysis of three-dimensional tumor-embedded breast models with different breast density compositions*, Med. Biol. Eng. Comput., pp. 1-11.
- [9] Bakhvalov, N., Panasenko, G., 1989, *Homogenisation: Averaging Processes in Periodic Media*. Kluwer Academic Publishers, Dordrecht .
- [10] Sanchez-Palencia, E., 1980, *Non-Homogeneous Media And Vibration Theory*, 127. Springer-Verlag, Berlin.
- [11] RamírezTorres, A., Grillo, A., Preziosi, L., RodríguezRamos, R., BravoCastillero, J., GuinovartDíaz, R., Sabina, F.J., 2017, *Thermal distribution in cancerous breast with anisotropic properties via a semi-analytical homogenization approach*. AIMETA 2017 Proceedings of the XXIII Conference of the Italian Association of Theoretical and Applied Mechanics. Edited by L. Ascione, V. Berardi, L. Feo, F. Fraternali, and A. M. Tralli. ISBN: 978-889-42484-7-0.
- [12] RamírezTorres, A., RodríguezRamos, R., Conci, A., Sabina, F. J., GarcíaReimbert, C., Preziosi, L., Merodio, J., Lebon, F., 2017, *A Semi-Analytical Heterogeneous Model for Thermal Analysis of Cancerous Breasts in Ng, E. Y. & Etehadtavakol, M.*, Application of Infrared to Biomedical Sciences, Springer Singapore, pp. 175-190.
- [13] Ng, E. Y. and Sudharsan, N. M., 2001, *An improved three-dimensional direct numerical modelling and thermal analysis of a female breast with tumor*. Proceedings of the Institution of Mechanical Engineers, Part H: Journal of Engineering in Medicine, 215(1), pp. 25-37.
- [14] Amri, A., Saidane, A. and Pulko, S., 2011. *Thermal analysis of a three-dimensional breast model with embedded tumour using the transmission line matrix (TLM) method*, Comput. Biol. Med. 41 (2), pp. 7686.
- [15] Cetingul, M. P. and Herman, C., 2010, *A heat transfer model of skin tissue for the detection of lesions: Sensitivity analysis*, Physics in Medicine and Biology, 55(19), pp. 59335951.
- [16] Bardati, F., Iudicello, S., 2008, *Modeling the visibility of breast malignancy by a microwave radiometer*, IEEE Trans. Biomed. Eng. 55 (1), pp. 214-221.
- [17] Gautherie, M., 1980. *Thermopathology of breast cancer: measurement and analysis*. Ann. N. Y. Acad. Sci., pp. 383-415.

- [18] Penta R, Ambrosi D, Quarteroni A, 2015. *Multiscale homogenization for fluid and drug transport in vascularized malignant tissues*, Mathematical Models and Methods in Applied Sciences. 25(01):79-108.
- [19] Penta R, Ambrosi D, 2015. *The role of the microvascular tortuosity in tumor transport phenomena*, Journal of theoretical biology. 364:80-97.
- [20] Mascheroni P, Penta R, 2017. *The role of the microvascular network structure on diffusion and consumption of anticancer drugs*, International journal for numerical methods in biomedical engineering. 33(10):e2857.
- [21] Shipley RJ, Chapman SJ, 2010. *Multiscale modelling of fluid and drug transport in vascular tumours*, Bulletin of mathematical biology. 72(6):1464-91.